ACS APPLIED MATERIALS & INTERFACES

Research Article

www.acsami.org

Facile Fabrication of Polymerizable Ionic Liquid Based-Gel Beads via Thiol−ene Chemistry

Mona Taghavikish, Surya Subianto, Naba Kumar. Dutta,* and Namita Roy Choudhury*

Ian Wark Research Institute, Mawson Lakes Campus, University of South Australia, Mawson Lakes, Adelaide, South Australia 5095, Australia

Supporting Information

ABSTRACT: Multipurpose gel beads prepared from natural or synthetic polymers have received significant attention in various applications such as drug delivery, coatings, and electrolytes because of their versatility and unique performance as micro- and nanocontainers.[1] However, comparatively little work has been done on poly(ionic liquid)-based materials despite their unique ionic characteristics. Thus, in this contribution we report the facile preparation of polymerizable ionic liquid-based gel beads using thiol−ene click chemistry. This novel system incorporates pentaerythritol tetra (3-mercaptopropionate) (PETKMP) and 1,4-di(vinylimidazolium) butane bisbromide in a thiol−ene-based photopolymerization to fabricate the gel beads. Their chemical structure, thermal and mechanical properties have been investigated using Fourier transform infrared spectroscopy (FTIR), differential scanning calorimetry (DSC), thermogravimetric analysis (TGA), and dynamic mechanical analysis (DMA). The gel beads possess low T_g and their ionic functionalities attribute self-healing properties and their ability to uptake small molecules or organic compounds offers their potential use as pH sensing material and macrocontainers.

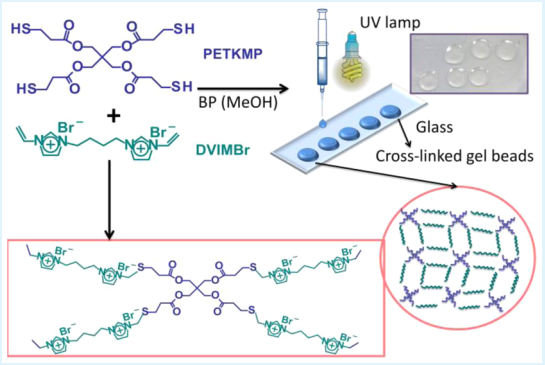

KEYWORDS: *polymerizable ionic liquid, gel beads, thiol−ene chemistry, self-healing, pH sensing material*

INTRODUCTION

Poly(ionic liquids) or polymerized ionic liquids (PIL) are a special class of polyelectrolyte with an ionic species in each of its repeating units. They have attracted significant interest because of the unique combination of properties of ionic liquids (IL) with a macromolecular architecture.[2,3] As polyelectrolyte gels, they have shown potential not only in more obvious applications such as electrolytes for batteries and supercapacitors,[4] but also where immobilization of active ingredients and their subsequent release in controlled fashion is desired, such as in drug delivery,[5] agriculture, and biomedical fields.[6] Indeed, they are showing a multitude of characteristics that make them very versatile materials with tunable properties.

Another characteristic of these PILs, that has not been well investigated is their potential self-healing capability: upon damage, the self-healing process requires either a suitable chemistry to trigger at the crack plane or exploit the in-built ability of the polymer network structure to repair macroscopic defects. This can occur via a molecular mechanism such as hydrogen bond or ionic interactions combined with physical processes such as viscoelastic flow (chain mobility and entanglement).[7,8] All these requisite characteristics for self-healing are found in PILs, as they are soft, polymeric materials that may have sufficient viscoelastic flow and also secondary ionic interactions to hold them together. However, very few investigations have been reported so far into the self-healing characteristics of PILs, and most of these studies have been directed toward the use of microcapsule or nanocontainers,[9] with scant reports on polymerizable ionic liquid-based gel beads.

Such gel beads have several attractive features for use in applications such as multifunctional additives: they are able to uptake liquids and active organic compounds, are chemically inert and stable, and possess tunable properties. One potential application for such PIL-based gel beads would be in anticorrosion coatings. Imidazolium-based ILs exhibit excellent inhibition performance on copper, steel and aluminum.[10,11] The actions of such inhibitors are correlated to the specific interaction of the −C═N− group of ILs and electronegative nitrogen in the molecule.[12] However, the main challenges in the use of IL are the risk of gradual loss over time and lack of miscibility. Xiong and co-workers[13] reported a facile one-step synthetic strategy for the preparation of cross-linked polymeric nanogels by the conventional radical copolymerization of a phosphonium-based IL for use as catalysts, whereas Muldoon and Gordon[14] reported the synthesis of polymer microgel by emulsion polymerization. However, no investigation has been reported on PIL micro gel beads for sensing and inhibition of corrosion.[15]

Received: May 21, 2015
Accepted: July 14, 2015
Published: July 14, 2015

DOI: 10.1021/acsami.5b04405
ACS Appl. Mater. Interfaces 2015, 7, 17298−17306

With a view to prepare such multipurpose gel beads with inhibitor or pH sensing (indicator) characteristics, we have chosen in this work thiol−ene based click chemistry to prepare PIL gel beads. The use of thiol−ene chemistry offers the desirable features of a click-type reaction and is frequently photo initiated.[16,17] This inherent versatility of thiol−ene chemistry allows for the reaction between a large variety of compounds that contains thiols with those containing unsaturated C═C groups, allowing a large degree of control on the macromolecular structure.[18] We herein report a thiol−ene photopolymerization using vinyl-containing imidazolium ionic liquids to prepare cross-linked gel beads under mild reaction conditions (Scheme 1). Combining the functionalities of thiol−ene and PIL chemistry, our aim is to create unique polymeric networks possessing multiple functionalities that are applicable toward anticorrosion coatings.

Scheme 1. Schematic of the Thiol−ene Photopolymerized Gel Beads Fabricated in This Study

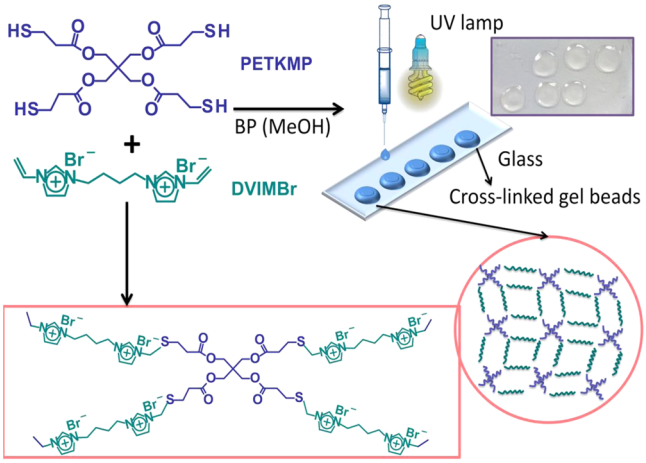

EXPERIMENTAL SECTION

Materials. Pentaerythritol tetrakis(3-mercaptopropionate) (PETKMP), 1-Vinylimidazole, 1,4-dibromobutane, benzophenone (BP), 1-butyl-3-methylImidazolium hexafluorophosphate, Azobis-(isobutyronitrile) (AIBN), methyl red, diethyl ether and methanol (analytical grade) were all obtained from Sigma-Aldrich, Australia and used without further purification. Double distilled water was used for all experiments.

Synthesis of 1,4-Di(vinylimidazolium)butane Bisbromide. 1,4-di(vinylimidazolium)butane bisbromide (DVIMBr) was synthesized by stirring a mixture containing 2:1 molar ratio of 1-vinylimidazole to 1,4-dibromobutane in methanol at 60 °C for 15 h. After cooling, the reaction mixture was added dropwise into 1 L of diethyl ether. The white precipitate was filtered off and dried at room temperature until constant weight with a yield of 68%.[19]

^{1}H NMR (300 MHz, D_2O, δ, ppm): 8.98 (2H), 7.69 (2H), 7.49 (2H), 7.04 (2H), 5.75 (2H), 5.33 (2H), 4.21 (4H), 1.87 (4H) (Figure S1).

Fabrication of Gel Beads. Gel beads were prepared using the slow solvent evaporation method using different ratio of precursors. In a typical synthesis method, a 1:2 mol ratio of pentaerythritol tetrakis(3-mercaptopropionate) (PETKMP) (0.5 mmol, 0.24g) and DVIMBr (1 mmol, 0.4 g) were dissolved in the minimum volume of methanol (0.2 mL) and small amount of BP (18.2 mg, 5 wt % with respect to monomer concentration). The reaction mixture was stirred for approximately 30 min in 4 mL vial while protecting from light and then ultrasonicated in the ice bath for 10 min with amplitude of 50%. The solution was then degassed in the degassing vacuum chamber while stirring for 1 h. Photopolymerization was initiated using an UV lamp in a dark hood. The gel beads were disposed drop by drop on a glass slide using a flat end needle (17 gauge, 1.07 mm inner diameter) syringe and beads were formed by exposure to UV light (365 nm wavelength). Transparent gel particles with an average size of 5 mm formed within 5 min. The beads were washed with water and methanol to remove any unreacted monomer; afterward, they were dried under a high vacuum. Elemental analysis shows: C, 40.6; S, 9.1; N, 7.9%. Calcd: C, 41.5; S, 9.8; N, 8.6%). Using this procedure, gel beads were also synthesized at two other 1:1 and 1:4 stoichiometric ratios of PETKMP:DVIMBr.

Characterization. ^{1}H NMR analysis was performed on a 300 MHz Bruker Avance spectrometer at room temperature using D_2O as the solvent. Infrared spectra of the gels were acquired using Nicolet Magna-IR Spectrometer 750 in photoacoustic mode, with 256 scans and using a carbon black reference. Differential scanning calorimetry (DSC) measurement was conducted using TA Instruments Discovery DSC (model 2920). The instrument was calibrated for baseline and cell constant prior to running the experiments. The samples were sealed in hermetic aluminum pans for use in the DSC experiment, and an empty pan was used as the reference. The temperature range for the experiment was from −70 to 200 °C, with a heating rate of 10 °C/min and under controlled nitrogen gas flow rate of 50 mL/min. For kinetic study the samples were held isothermally at 125, 135, and 145 °C for 45 min under a flow of nitrogen. Thermogravimetric analysis (TGA) was performed using a TA Instruments Discovery TGA with an

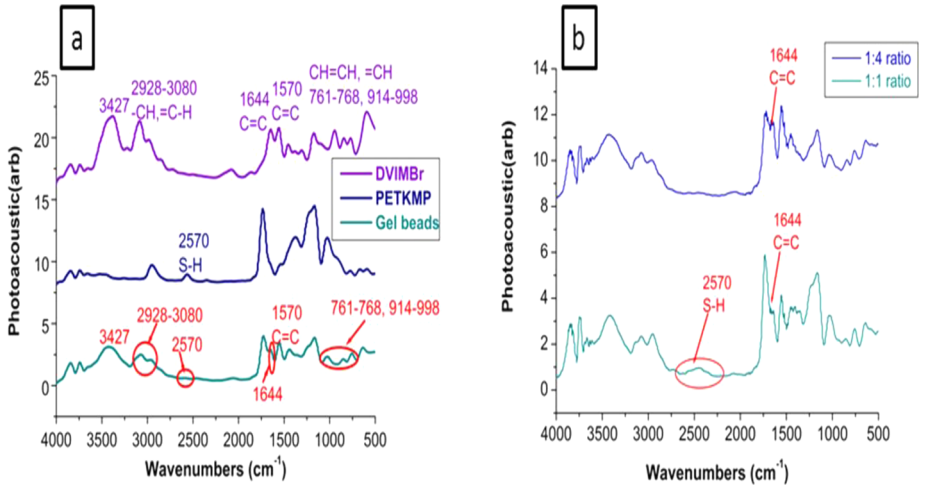

Figure 1. (a) FTIR spectra of the cured gel beads with stoichiometric (1:2) ratio of the monomers used, (b) FTIR spectra of 1:1 and 1:4 ratios.

DOI: 10.1021/acsami.5b04405
ACS Appl. Mater. Interfaces 2015, 7, 17298−17306

aluminum pan. The samples were subjected to a 10 °C/min ramp rate from 100 to 550 °C under a nitrogen atmosphere. The UV−vis experiment was carried out with Evolution 201 UV/vis spectrophotometer. Qsonica ultrasonicator was used for ultrasonication. Elemental analysis was performed using a LECO Trumac CNS analyzer. DMA was conducted using the TA Instruments Q800 DMA equipped with a humidity accessory. The storage and loss moduli of the gel samples were determined under controlled humidity. The gel strips of thickness of 1.3 mm and width of 9.3 mm were mounted using a tension clamp and run at ambient temperature with amplitude of 10 μm and a preload force of 0.0100 N. The DMA run was conducted with the humidity ramped to 75% and held for the duration of half an hour with isothermal temperature. Rheometric measurements were performed on an ARES (TA Instruments) AR-1000 Rheometer using parallel plate geometry. All tests were done at room temperature with light intensity around 90 mW cm^{-2}. The rheometer was operated at a frequency of 0.3 Hz with average strain amplitude of 1%.

RESULTS AND DISCUSSION

Thiol−ene Photopolymerization. FTIR analysis of the cured gel beads with stoichiometric ratio shows the disappearance of the reactants after photo polymerization for 5 min. As can be seen in Figure 1a, the spectra of the monomers (DVIMBr and PETKMP) show distinct differences with the cured gel beads. The spectrum of DVIMBr shows various characteristic peaks associated with the ionic liquids structure and the unsaturated vinyl moiety. It shows two bands at 3080 (=C−H stretching) cm^{-1} and at 2928 cm^{-1} representing the stretching of −CH groups of the imidazole ring of the IL, a peak for the C=C double bonds of the imidazole ring around 1570 cm^{-1}, and another for the C=C stretching of the vinyl group at 1644 cm^{-1}. It also shows the presence of bands attributed to the vinyl group between 914 and 998 (out-of-plane =C−H bending) and at 761−768 cm^{-1} (H−C=C−H wagging). The spectrum of the other monomer, PETKMP, shows presence of a peak attributed to thiol groups at 2570 cm^{-1}(S−H stretching). The cured PIL gel beads, on the other hand, show no detectable amount of the peak due to sulfur−hydrogen stretching around 2570 cm^{-1} as well as the absence of the C=C vinyl peak at 1644 cm^{-1}, which indicates that the thiol and vinyl groups have fully reacted. A reduction in intensity at 3080 cm^{-1} and around 761−768, 914−998 cm^{-1} regions in gel beads spectra in comparison with the DVIMBr spectra also confirms the consumption of vinyl groups. Additionally, there is also a band at 3427 cm^{-1} in the spectra of the PIL gel (which was also present in the DVIMBr spectra) which is attributed to strongly bound water. This analysis was supported by elemental analysis, which confirmed a 1:2 ratio of sulfur to nitrogen in cured gel beads, which is in agreement with the stoichiometry used for the fabrication of these gel beads.

In PIL gels, conversion rate and the extent of cross-linking is important as the toughness of such material depends on these parameters. As such, the stoichiometry between the thiol and vinyl groups (monomer ratio) and polymerization time (extent of cross-linking) are the vital factors for controlling the material's properties through achieving a high monomer conversion and preventing side reactions.[20] Thus, in addition to the 1:2 ratio, we have fabricated samples with a 1:1 (excess thiol groups) and 1:4 (excess vinyl groups) ratio of PETKMP:DVIMBr to investigate the effect of stoichiometry on the PIL gel formation. As can be expected, FTIR spectrum of sample with 1:1 ratio (Figure 1b) shows an extra S−H group but full consumption of the C=C vinyl peak because there are extra thiol groups available, whereas in the sample with a 1:4 ratio where excess vinyl groups were used, there is no evidence of unreacted thiol groups (Figure 1b) but evidence of excess, unreacted vinyl group. This indicates that although in principle homopolymerization of DVIMBr could occur as a competing reaction to the thiol−ene reaction, the FTIR spectrum shows that the thiol−ene reaction occurs in preference and thus the excess vinyl groups did not lead to extensive homopolymerization of DVIMBr after all the thiol have been consumed. This approach offers us the advantage to prepare either excess thiol functionalized or excess vinyl functionalized (off-stoichiometry) thiol−ene-based gel beads (e.g oligomeric IL gel with excess vinyl group) for further modification.

Kinetics of Thiol−ene Reaction. *In Situ Dynamic Rheology during Photopolymerization.* Direct monitoring of the thiol−ene reaction and cross-linking was done by in situ rheology. Under UV light exposure, the shear modulus changes were followed as reaction progressed to understand the effect of stoichiometry on the thiol−ene reaction. When the stoichiometric amounts (1:2) were used, it can be seen that the elastic modulus G' and the viscous modulus G'' increase significantly after 30 s and starts to plateau after 2 min, indicating a very rapid reaction (Figure 2). As observed in Figure 2, the step

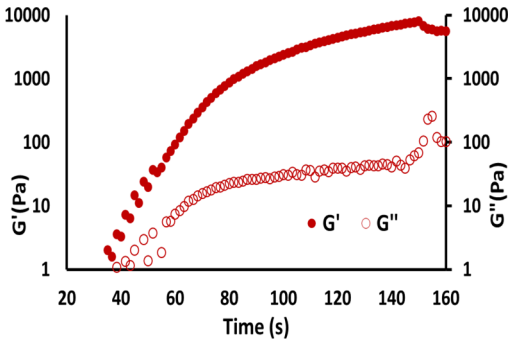

Figure 2. In situ rheology study during photopolymerization of the PETKMP:DVIMBr system (1:2 ratio).

growth polymerization proceeds rapidly achieving a modulus value of ∼10 kPa within 3 min of light exposure. Also, both the G' and G'' increased at about the same point in time, however the crossover point could not be seen as expected for a fully gelled sample, but noise appeared in data after 2 min, with the values fluctuating strongly after 140s due to drying of the solvent. A plateau in G' curve gives an indication of approximate reaction time for the photopolymerization of the system. This seems to indicate that under shear conditions, although the thiol−ene reaction took place the applied shear may have prevented the formation of a solid, cohesive gel, but rather a loosely attached dispersion of gelled material within the solvent (methanol). Nevertheless, it confirmed that the thiol−ene reaction occurred rapidly at room temperature under UV irradiation.

As can be seen from Figure 3, increasing either the DVIMBr or PETKMP content (excess vinyl or thiol) resulted in a slower gelation compared to the stoichiometric ratio sample (1:2). The addition of excess thiol (1:1) resulted in a material with a lower modulus compared to the stoichiometric ratio, while increasing the vinyl content resulted in a material which ultimately may have greater modulus; however the polymerization was slower and more gradual as it is likely to be a

DOI: 10.1021/acsami.5b04405
ACS Appl. Mater. Interfaces 2015, 7, 17298−17306

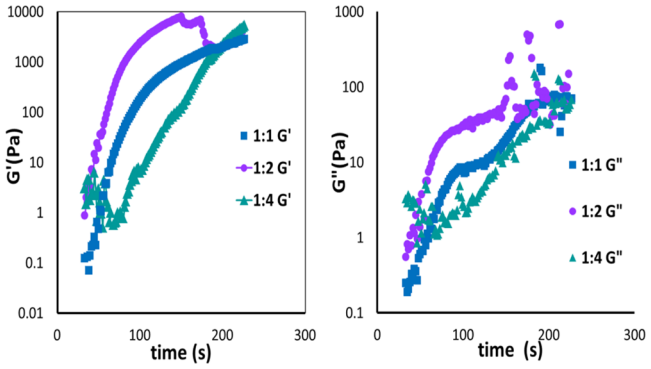

Figure 3. In situ rheology study during photopolymerization of PETKMP/DVIMBr of varying stoichiometry showing evolution of mechanical properties.

mixture of thiol−ene reactions and free radical polymerization. In each case, it led to the formation of polymer or oligomer with excess thiol or vinyl groups.

Kinteic Study of Photopolymerization Using Differential Scanning Calorimetry. On the basis of the above results, the stoichiometric amount of 1:2 of PETKMP:DVIMBr was chosen as an optimal composition for further kinetic study. In this case the kinetics of the thiol−ene reaction was further studied using differential scanning calorimetry (DSC) by both a temperature-ramp and isothermal methods.[21] In this work, a thermal initiator (AIBN) was used for a comparative study with photoinitiated system. However, as thiol−ene chemistry proceeds through a radical step-growth mechanism, it was expected that experiments with thermal initiator would yield similar trends to the photoinitiated system.

To do this, first two conventional DSC experiments (with a temperature ramp) were performed to find the effective thiol−ene curing temperature: first using the divinyl monomer only (DVIMBr) with thermal initiator (AIBN) (to find the divinyl polymerization temperature range) and second using the full stoichiometric polymerization system with monomers, solvent, and thermal initiator (DVIMBr/PETKMP/MeOH/AIBN). In the first experiment, the DVIMBr polymerization reaction was detected at 396 K, whereas in the second experiment, a broad peak from 398 to 423 K indicates the occurrence of thiol−ene reaction.

On the basis of these results, the kinetics of the thiol−ene reaction was then studied using an isothermal method where the samples were quickly brought to a temperature above which the reaction starts and held isothermally, monitoring the course of polymerization over time. Thus, the sample is quickly brought to one of three different temperatures within the appropriate temperature range (398, 408, and 418 K) at a fast heating rate of 20 K/min (the fast ramp rate was used to minimize the effect of the heating ramp), and then held at that temperature for a fixed time (45 min). The time duration and the enthalpy (ΔH) were then determined from the DSC isothermal exotherm for all three temperatures. As shown in Figure 4a, the peak maximum occurs more rapidly with increasing temperatures. The presence of the maximum in the reaction curve indicates that the reaction follows an autocatalytic mechanism, while the heat evolved during polymerization reaction at a particular time is directly proportional to the degree of conversion ($x = \Delta H_1/\Delta H$).

From these data, the values can then be converted to a reaction rate (k), $d\alpha/dt$, using an isothermal conversion (%) vs time (min) graph. The calculated values were then used to plot $\ln[k(T)]$ versus $1/T$ (Arrhenius plot), which indicates that the thiol−ene reaction is a zero order reaction as the plot was linear (Figure 4b). Because the fit of the line follows the equation $\ln K = \ln Z - E_a/RT$, the value of the reaction constant K can be determined from the y value of the fitted experimental data, whereas the slope of the fit is equal to E_a/R (as $1/T$ is set as the x values) and the intercept is equal to Ln Z. Using this equation the activation energy (E_a) of 8.54 kJ/mol and pre-exponential factor (Z) of 107.5 S^{-1} are obtained from the slope and intercept of this plot, respectively. Previously, Cook and co-workers[22] reported the activation energy for photopolymerization of thiol−ene reaction is 7.6 kJ/mol, which is in very good agreement with the results reported here. This low value of activation energy for free radical polymerization corresponds to the fact that the thiol−ene reaction is a very fast reaction with the activation energy of the initiation step being close to zero.

Thermal and Mechanical Study. *Thermal Behavior Using Thermogravimetric Analysis.* Thermogravimetric analysis was done on the gel beads to confirm the formation of the polymer and study the properties of the gel beads. The TGA of the cured gel beads (Figure 5) showed one main degradation (around 70 wt %) with an onset temperature of around 265 °C and peak degradation temperature of 313 °C, with the gradual weight loss above 360 °C likely due to sulfur-containing residues. Previous literature on similar, nonpolymerized imidazolium ionic liquid with Br^- counterion reported an onset of degradation at around 253−259 °C. Comparatively, this 10 °C increase in thermal stability of the PIL gel beads is

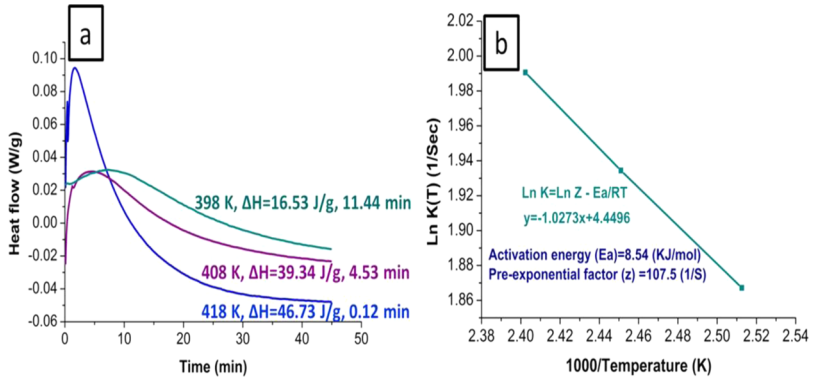

Figure 4. (a. Isothermal exotherm of PETKMP/DVIMBr system at three different temperatures measured using DSC, (b) Arrhenius plot of the DVIMBr/PETKMP system.

DOI: 10.1021/acsami.5b04405
ACS Appl. Mater. Interfaces 2015, 7, 17298−17306

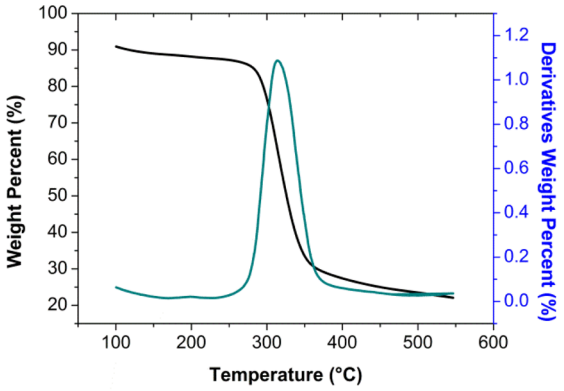

Figure 5. TGA thermogram of the gel beads (1:2 ratio) showed in black and first derivatives vs temperature presented in dark cyan.

ascribed to the photopolymerised PIL.[23] This is supported also by the higher range of temperature at which the main degradation occurs, with gel beads showing the thermal degradation over 265−350 °C, whereas free ionic liquid was completely degraded at around 330 °C. The existence of only a single degradation peak also indicates that there are unlikely to be unreacted reagents or small molecular weight oligomers present (as this would show a lower onset degradation temperature, resulting in a second mass loss earlier than the main degradation). The TGA also indicates that there is trace amount of water present in the gel beads as there is a gradual mass loss at 100−150 °C, which confirms our previous FTIR results showing a peak for tightly bound water molecules.

The thermal degradation properties were also affected by the stoichiometry. Comparing the TGA thermograms in Figure 6

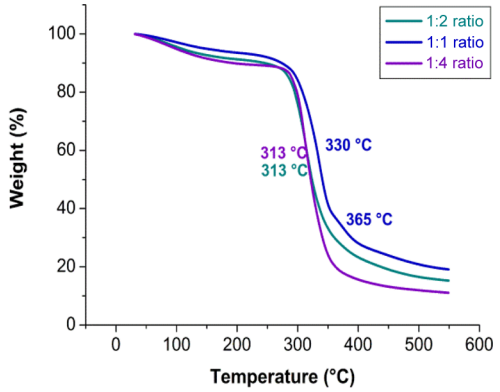

Figure 6. TGA thermogram showing the peak degradation temperature of three samples with different stoichiometric ratios of PETKMP:DVIMBr (1:2, 1:1, 1:4).

of samples with different stoichiometry (1:1, 1:2, 1:4 molar ratios of PETKMP and DVIMBr), samples with a 1:1 ratio show an earlier onset of degradation that is ascribed to the unreacted thiols (which is a liquid) volatizing at their boiling point of around 275 °C. Also, two peak degradation temperatures were observed in the 1:1 ratio sample at 330 and 365 °C, whereas the 1:2 and 1:4 ratio samples show only one peak degradation around 313 °C. This confirms our assignment of the main degradation to the degradation of the PIL gel and the second one to the degradation of sulfur-containing residues, as this second degradation increases with increasing amount of thiols (1:1 > 1:2 > 1:4 stoichiometry). The excess thiols may have reacted at these temperatures to form other compounds which resulted in the slight shift of the peak degradation temperature in this sample (1:1 ratio). On the other hand, 1:2 and 1:4 showed almost same degradation profile as a result of the same kind of product in their structure because of the thiol−ene reaction, as further homopolymerization of DVIMBr in 1:4 ratios is unlikely to significantly affect the thermal degradation temperature.

Phase Behavior Study Using Differential Scanning Calorimetry. In this type of gel material, another parameter of interest is the glass transition temperature (T_g). This is because self-healing in this type of material occurs through a combination of intermolecular diffusion and reversible, dynamic noncovalent bonds. DSC thermogram of samples with varying stoichiometry is shown in Figure 7. DSC results in Figure 7

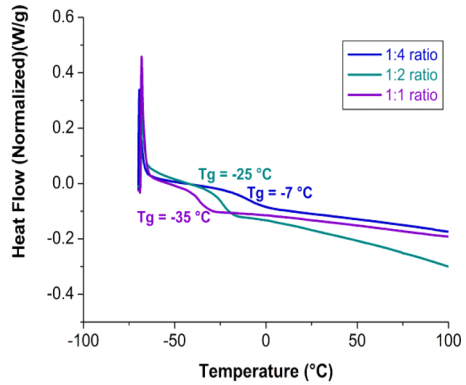

Figure 7. DSC thermogram showing the glass transition temperature of three samples with varying stoichiometry of PETKMP:DVIMBr (1:1, 1:2, 1:4) under a temperature ramp of 10 °C/min.

show that sample containing excess thiol (1:1 ratio) has the lowest T_g around −35 °C which is almost same as the Tg of the DVIMBr monomer. This shows that there were insufficient amount of cross-linkable vinyl groups to form an extensive thiol−ene network and thus only low molecular weight oligomers were formed where they are likely to be held together by ionic interaction rather than extensive physical entanglement. It is worth noting that this sample disintegrated when immersed in water, which indicates a loose network formation. On the other hand, increasing the PETKMP:DVIMBr ratio to the required stoichiometric amounts or to an excess in vinyl groups increases the T_g, with a T_g of −25 °C for the 1:2 ratio sample and increasing to around −7 °C in the 1:4 ratio sample, indicating strong network formation. The higher T_g for the sample with excess vinyl group (1:4) compared to the stoichiometric one (1:2) indicates the occurrence of some homopolymerization of the vinyl monomer; however, as was shown in the FTIR results previously, the main process for the network formation was the thiol−ene reaction.

Nevertheless, low T_g materials allow interchain diffusion and entanglement at room temperature,[24] resulting in a degree of self-healing based on two mechanisms; reconstruction of noncovalent bond by hydrogen bonding or reassociation of the molecular chain as proposed by Wool and O'Connor.[25] In this mechanism, diffusion of polymer chains near the surface results in the displacement and entanglement of mobile chains followed by interpenetration into the matrix material, healing the initial defect or rupture. Previous studies on elastomers show that this occurs mainly at temperatures above the bulk

DOI: 10.1021/acsami.5b04405
ACS Appl. Mater. Interfaces 2015, 7, 17298−17306

polymer glass transition temperature (T_g), and Scheltjens et al.[26] reported that with increasing mobility (by reducing T_g) the self-healing properties can be improved.

To investigate the autonomous self-healing properties of this composition at ambient environment, we cut the gel beads (1:2 ratios) using scalpel and the healing process was observed with a high speed camera. Figure 8 inset shows the time laps optical image of healing behavior of cut sample surface. It is clear that upon the occurrence of microcracks at room temperature, the gel beads have sufficient chain mobility, allowing them to flow into and fill small gaps to recover the surface in a healing process. This is evidenced by time lapse images of a scratch on the surface of the gel beads, which show that the material is capable of viscoelastic flow into such defects (Figure 8), and thus demonstrating a degree of self-healing behavior in the bulk material. As such, the gel beads are an intrinsic type of self-healing materials with an internal ability for repair to occur through molecular-scale mechanisms, such as polymer-chain mobility and entanglement. Such a mechanism is reversible, making multiple healings possible.

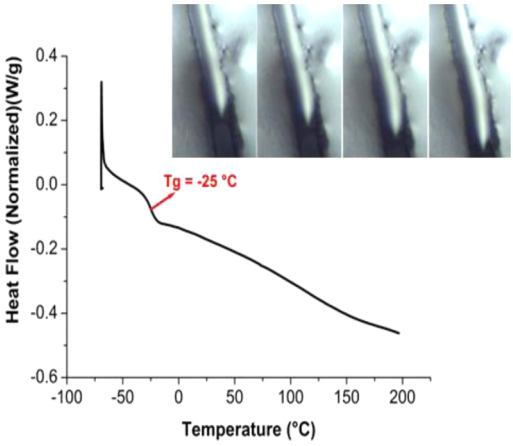

Figure 8. DSC thermogram of the cured gel beads (1:2 ratios). Inset: time-lapse optical image of healing on a cut on the surface of a gel bead.

Mechanical Properties of the Gels by Dynamic Mechanical Analysis (DMA). DMA is a useful tool to obtain the viscoelastic properties of these ionic gels. Generally, it has been reported that thermal and mechanical parameters are directly related to features inherent to the chemical structure of both the thiol and ene functional groups.[27] To provide corroborative evidence for the DSC results and provide an interpretation of those results, the dynamic mechanical test was conducted. Figure 9 shows the storage modulus (E) data at different ratios and at two different humidity levels (40 and 60% relative humidity) at room temperature. It shows a significant increase in the storage modulus from 0.054 MPa for 1:1 ratio to 7.7 MPa for 1:2 and 19.88 MPa for 1:4 ratios at 40% humidity. The low modulus for the sample with 1:1 ratio confirms the lack of network formation in this sample, while the increase between the 1:2 and 1:4 also shows some homopolymerization of DVIMBr can occur after the thiols have been reacted. At 60% humidity level, an increase in modulus was detected with increasing DVIMBr content but in the case of 1:4 ratio samples, breakage occurred. This is consistent with the DSC results in Figure 8, where increased T_g for this sample may make it more brittle.

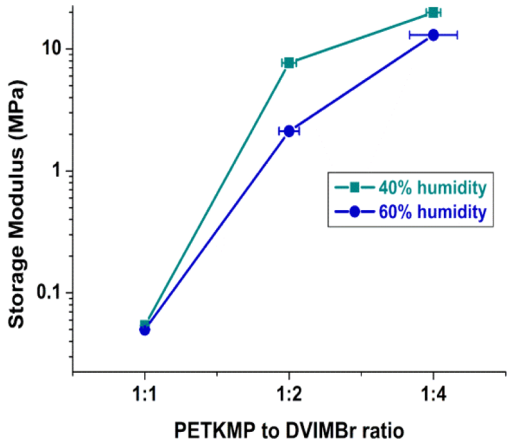

Figure 9. Storage modulus of three different ratios of thiol−ene reaction in two different humidity levels. The sample with 1:4 ratio did not fully maintain its mechanical integrity and broke during measurement so the value for 1:4 ratio at 60% is the last record.

The DSC and DMA results indicate that in the 1:1 ratio, the structure is likely that of a loosely bound network with greater coordinated segmental motion and as a result has the least mechanical strength and lowest T_g. The sample with 1:2 ratio appears to have optimized full network formation, resulting in higher T_g and modulus. This sample also shows more stable mechanical properties, which is decreased slightly with increasing humidity but remained intact, whereas the sample with a 1:4 ratio (with the highest modulus) breaks because of its brittle nature.

On the basis of the previous results, it is clear that three different precursor ratios lead to different compositions of polymer with different characteristics. The 1:1 system mostly showed oligomeric type behavior, whereas 1:2 was a fully cross-linked network and 1:4 was more brittle, with a mixture of both thiol−ene and vinyl polymerized systems.

Thus, the stoichiometric ratio of 1:2 of PETKMP:DVIMBr was considered optimal as it provides a material that is thermally and mechanically more stable and robust. This material is then selected for studying further for its use as a reservoir for controlled release or delivery.

Poly(Ionic Liquid) Gels as pH Sensing Material. Although it has not been widely studied in anticorrosion applications, another characteristic of PILs is that they contain ionic functionalities which can bind ionic compounds through ion exchange. Similar materials have been shown in the literature[10] to be able to act as corrosion indicators; when loaded with pH sensing molecule and incorporated into coatings, this adds significant value and a diagnostic aspect to the coating. It is expected that this PIL gel would be able to perform similar task, and thus a preliminary sorption study was done using these gels. In this study a pH indicator, methyl red (MR), was incorporated into the gel through ion exchange. The synthesized gels are placed into a solution containing 0.3 wt % of MR and the uptake of dye into the gel was monitored by UV−vis spectroscopy through the decrease in the color intensity of the dye solution. After 9 days, no further reduction in color intensity was observed, which indicates that the dyes have been absorbed into the beads (Figure S2). The unbound dyes were then washed from the beads by soaking the beads in ultrapure water (Figure S3). The release of unbound dyes during 16 days was also monitored through UV−vis (Figure

DOI: 10.1021/acsami.5b04405
ACS Appl. Mater. Interfaces 2015, 7, 17298−17306

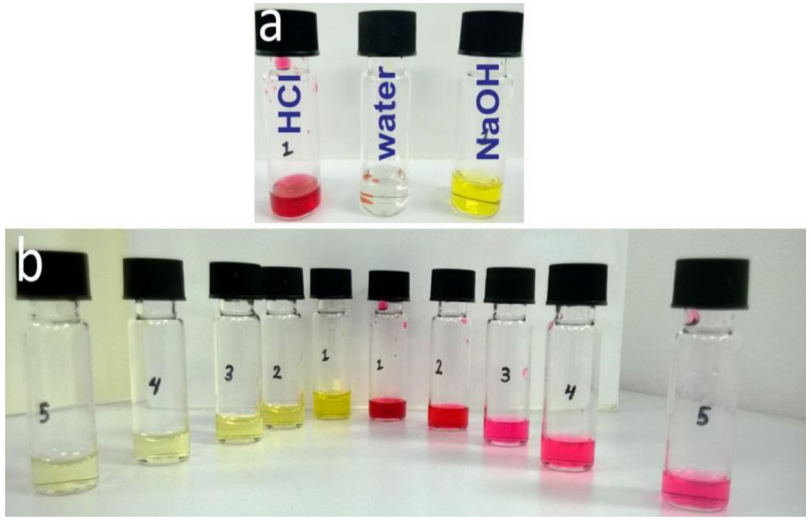

Figure 10. (a) Indicator (MR) release from the gel beads due to pH changes; (b) successive leaching showing that after 5 repetitions, leaching of MR was still observed.

S4), and after 16 days, the peak intensity in the UV−vis spectra reached a plateau (Figure S5), indicating all the unbound dyes have been washed out. Since the gel beads themselves remained strongly colored after washing, this indicates that the remaining dye within the gel is bound through ionic interaction with the vinylimidazolium moiety.

This was confirmed by the fact that when the washed, MR loaded−beads were exposed to ultrapure water at neutral pH, no visible leaching of MR was observed. However, as soon as the pH of the surrounding aqueous medium was lowered (pH ∼ 0.5) by adding 0.1 M HCl (pK_a of methyl orange is 5.1), slow release of MR into water was observed by changing of the solution color to pink (Figure 10a). This was confirmed through UV−vis measurements (Figure S6) that show a quick release of MR into solutions of 0.1 M HCl or 0.1 M NaOH; however, there was no release detected in deionized water over 24 h. This shows that unlike a container that relies on physical entrapment, the PIL gel acts as an active, environmental sensing container where the release of the indicator dye is controlled by the pH of the solution. This is because the MR is bound in the PIL gel through ion exchange, and a lowering in pH changes the nature of the MR by protonating the carboxylate ion and, disrupting the ionic bond between the MR and the imidazolium group of the PIL and releasing the MR into the solution. Similarly, exposure to higher pH by adding 0.1 M NaOH releases MR into water through anion exchange with the hydroxyl ions, changing the solution color to yellow. This shows that the unique property of PIL gels enables both acidic and basic conditions to induce a slow release of pH indicators,[28] making it a versatile pH sensing material. The speed of the release is also suitable for the intended application in corrosion, as this would mean that the indicator would be released readily only when corrosion occurs.

Furthermore, although this release mechanism was pH sensitive, it was also sufficiently gradual to be repeatable several times. The leaching through pH change (by repeated washing and exposure to low/high pH) was repeated 5 times and even after this further release of bound MR could still be detected (Figure 10b), indicating that despite the rapid release of MR under acidic or basic conditions, sufficient MR was still retained in the PIL gel beads for sustained release. This may offer advantages in longevity compared to indicators directly incorporated in coatings,[10] as repeated use is possible, while still offering the advantages of mobility of the indicator molecules as opposed to immobilized approaches such as with covalently bound[29] or sol−gel-based systems.[30] These experiments show the potential of these gel beads as pH sensing indicators for applications such as environmentally friendly coatings, which will be investigated in future studies.

Ionic Liquid Gel as Macrocontainer for IL. To investigate whether these PIL gels have the potential to be used as macrocontainers for other compounds, we have examined them as containers for ionic liquid for potential anticorrosion application.[31−33] Unlike other encapsulation methods, these PIL-based macrocontainers may solve some of the drawbacks of traditional (nonpolymerized) IL gels such as phase mixing, phase separation, leakage of ionic liquids as well as the high viscosity of ionic liquids. Till now, studies have been conducted with ionic liquids in polymeric or inorganic macrocontainers, but there is little study on the use of PIL macrocontainers.[34]

In terms of potential applications in anticorrosion coatings, loading of corrosion inhibitors onto macrocontainers have shown promising results for corrosion protection.[35] Free ILs have been shown to act as corrosion inhibitors,[11] and PIL gel beads would be an ideal reservoir for ILs since they would have a high compatibility. Thus, the loading capacity of the PIL gel was investigated with respect to the feasibility of this approach. For this experiment, 1-butyl-2,3-dimethylimidazolium hexafluorophosphate ionic liquid (IL) was dissolved in tetrahydrofuran (THF) and preweighted PIL gel beads was added to the solution, and the mass uptake was monitored over 40 days through the weight changes of the gel beads. As can be seen in Figure 11, under ambient conditions the PIL gel beads gradually uptake free IL during 30 days, reaching a plateau after around 25% mass uptake. This uptake is quite linear for most of this time period, indicating a straightforward diffusion-controlled uptake of IL from solution. This uptake result is also supported by FTIR in Figure 12, which shows extra peaks at 852−559 cm^{-1} indicating the presence of the hexafluorophosphate of the free IL in the PIL gel beads. This 25% loading is relatively low compared to some encapsulation methods where IL acts as a solvent to a gelling agent,[36] but is comparable to IL uptake of materials with similar macromolecular structures such as polyelectrolyte membranes,[37] and this is attributed to the IL

DOI: 10.1021/acsami.5b04405
ACS Appl. Mater. Interfaces 2015, 7, 17298−17306

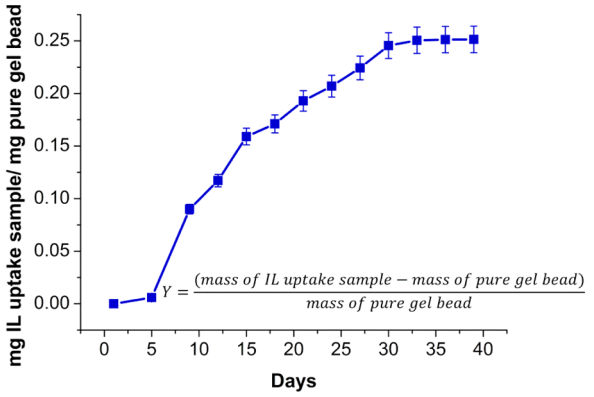

Figure 11. IL uptake of the gel beads where the *Y* axis is calculated using the above formulation and the *X* axis presents the number of days.

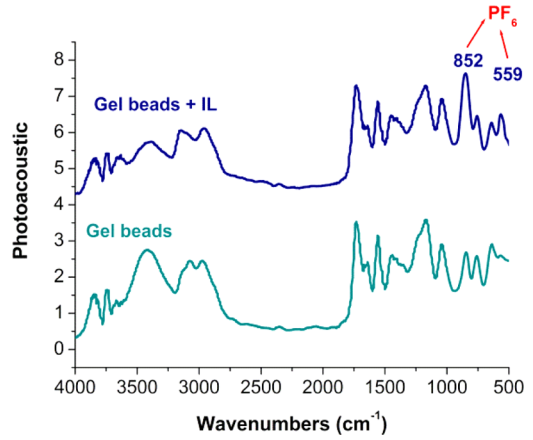

Figure 12. FTIR spectra of the IL-loaded gel beads.

being uptaken after synthesis rather than present during network formation.

In this study, the PIL gel beads are formed as a cross-linked network with methanol as the solvent, and this limits the maximum sorption of the bulky IL molecules post-synthesis. It is likely that reducing the cross-link density or having the IL acting as the polymerization solvent would significantly increase IL loading; however this is beyond the scope of the current study. This result does show that the PIL gel beads are able to act as macrocontainers for IL, with potential use in various applications such as anticorrosion coating.[11] Currently work is underway to investigate those behaviors and will be communicated in our future work.

CONCLUSION

In this work, we have shown the fabrication of poly(ionic liquid) gel beads through click-type reactions using thiol−ene chemistry. The use of thiol−ene chemistry allows for a very rapid and efficient formation of gel beads suitable for large scale synthesis. The formation of gel beads is confirmed through FTIR, thermal analysis, and kinetic studies. These gel beads also show self-healing characteristics, capable of reassociation of chains through viscoelastic flow into small defects, because of their rubbery nature. The beads also demonstrate the ability to uptake active molecules such as corrosion inhibitors or as macrocontainers for sensing molecules through ion exchange, with the ability to pH sensing or controlled release of active anticorrosion agents. Overall, these results show that these gel beads are multipurpose promising materials suitable for pH sensing or anticorrosion applications.

ASSOCIATED CONTENT

Supporting Information

The Supporting Information is available free of charge on the ACS Publications website at DOI: 10.1021/acsami.5b04405.

^{1}H NMR and experimental details of dye uptake and release study with UV−vis data (PDF)

AUTHOR INFORMATION

Corresponding Authors

*E-mail: naba.dutta@unisa.edu.au. Tel.: +6188302 3546.

*E-mail: namita.choudhury@unisa.edu.au. Tel.: +6188302 3719.

Notes

The authors declare no competing financial interest.

ACKNOWLEDGMENTS

The authors gratefully acknowledge the financial support of the Australian Research Council's Linkage grant for carrying out this work and also the industry partner Wave rider Energy for financial support of this work. The authors thank Mr. Steve Shamis of TA Instruments for assistance with the Photo-rheology work.

REFERENCES

(1) Priya James, H.; John, R.; Alex, A.; Anoop, K. R. Smart Polymers for the Controlled Delivery of Drugs − a Concise Overview. *Acta Pharm. Sin. B* **2014**, *4*, 120−127.

(2) Yuan, J.; Antonietti, M. Poly(Ionic Liquid)S: Polymers Expanding Classical Property Profiles. *Polymer* **2011**, *52*, 1469−1482.

(3) Shaplov, A. S.; Vlasov, P. S.; Lozinskaya, E. I.; Shishkan, O. A.; Ponkratov, D. O.; Malyshkina, I. A.; Vidal, F.; Wandrey, C.; Godovikov, I. A.; Vygodskii, Y. S. Thiol-Ene Click Chemistry as a Tool for a Novel Family of Polymeric Ionic Liquids. *Macromol. Chem. Phys.* **2012**, *213*, 1359−1369.

(4) Raghavan, P.; Manuel, J.; Zhao, X.; Kim, D.-S.; Ahn, J.-H.; Nah, C. Preparation and Electrochemical Characterization of Gel Polymer Electrolyte Based on Electrospun Polyacrylonitrile Nonwoven Membranes for Lithium Batteries. *J. Power Sources* **2011**, *196*, 6742−6749.

(5) Murata, Y.; Sasaki, N.; Miyamoto, E.; Kawashima, S. Use of Floating Alginate Gel Beads for Stomach-Specific Drug Delivery. *Eur. J. Pharm. Biopharm.* **2000**, *50*, 221−226.

(6) Kashyap, N.; Kumar, N.; Kumar, M. N. V. R. Hydrogels for Pharmaceutical and Biomedical Applications. *Crit. Rev. Ther. Drug Carrier Syst.* **2005**, *22*, 107−149.

(7) Xing, X.; Li, L.; Wang, T.; Ding, Y.; Liu, G.; Zhang, G. A Self-Healing Polymeric Material: From Gel to Plastic. *J. Mater. Chem. A* **2014**, *2*, 11049−11053.

(8) Cui, J.; Campo, A. D. Multivalent H-Bonds for Self-Healing Hydrogels. *Chem. Commun.* **2012**, *48*, 9302−9304.

(9) Blaiszik, B. J.; Sottos, N. R.; White, S. R. Nanocapsules for Self-Healing Materials. *Compos. Sci. Technol.* **2008**, *68*, 978−986.

(10) Maia, F.; Tedim, J.; Bastos, A. C.; Ferreira, M. G. S.; Zheludkevich, M. L. Nanocontainer-Based Corrosion Sensing Coating. *Nanotechnology* **2013**, *24*, 415502.

(11) Ibrahim, M. A. A.; Messali, M.; Moussa, Z.; Alzahrani, A. Y.; Alamry, S. N.; Hammouti, B. Corrosion Inhibition of Carbon Steel by Imidazolium and Pyridinium Cations Ionic Liquids in Acidic Environment. *Port. Electrochim. Acta* **2011**, *29*, 375−389.

DOI: 10.1021/acsami.5b04405
ACS Appl. Mater. Interfaces 2015, 7, 17298−17306

(12) Baskar, R.; Kesavan, D.; Gopiraman, M.; Subramanian, K. Synthesis of Novel Photosensitive Polymers for the Protection of Mild Steel from Acid Corrosion. *RSC Adv.* **2013**, *3*, 17039−17047.
(13) Xiong, Y.; Wang, H.; Wang, R.; Yan, Y.; Zheng, B.; Wang, Y. A Facile One-Step Synthesis to Cross-Linked Polymeric Nanoparticles as Highly Active and Selective Catalysts for Cycloaddition of Co2 to Epoxides. *Chem. Commun.* **2010**, *46*, 3399−3401.
(14) Muldoon, M. J.; Gordon, C. M. Synthesis of Gel-Type Polymer Beads from Ionic Liquid Monomers. *J. Polym. Sci., Part A: Polym. Chem.* **2004**, *42*, 3865−3869.
(15) Men, Y.; Kuzmicz, D.; Yuan, J. Poly(Ionic Liquid) Colloidal Particles. *Curr. Opin. Colloid Interface Sci.* **2014**, *19*, 76−83.
(16) Hoyle, C. E.; Lee, T. Y.; Roper, T. Thiol−Enes: Chemistry of the Past with Promise for the Future. *J. Polym. Sci., Part A: Polym. Chem.* **2004**, *42*, 5301−5338.
(17) Hoyle, C. E.; Bowman, C. N. Thiol−Ene Click Chemistry. *Angew. Chem., Int. Ed.* **2010**, *49*, 1540−1573.
(18) Gokmen, M. T.; Brassinne, J.; Prasath, R. A.; Du Prez, F. E. Revealing the Nature of Thio-Click Reactions on the Solid Phase. *Chem. Commun.* **2011**, *47*, 4652−4654.
(19) Yuan, J.; Antonietti, M. Poly(Ionic Liquid) Latexes Prepared by Dispersion Polymerization of Ionic Liquid Monomers. *Macromolecules* **2011**, *44*, 744−750.
(20) Storha, A.; Mun, E. A.; Khutoryanskiy, V. V. Synthesis of Thiolated and Acrylated Nanoparticles Using Thiol-Ene Click Chemistry: Towards Novel Mucoadhesive Materials for Drug Delivery. *RSC Adv.* **2013**, *3*, 12275−12279.
(21) Joraid, A. A.; Abu-Sehly, A. A.; Alamri, S. N. A Study on Isothermal Kinetics of Glassy Sb9.1te20.1se70.8 Alloy. *J. Taibah Univ Med. Sci.* **2009**, *2*, 106−117.
(22) Cook, W. D.; Chausson, S.; Chen, F.; Le Pluart, L.; Bowman, C. N.; Scott, T. F. Photopolymerization Kinetics, Photorheology and Photoplasticity of Thiol−Ene−Allylic Sulfide Networks. *Polym. Int.* **2008**, *57*, 469−478.
(23) Awad, W. H.; Gilman, J. W.; Nyden, M.; Harris, R. H., Jr; Sutto, T. E.; Callahan, J.; Trulove, P. C.; DeLong, H. C.; Fox, D. M. Thermal Degradation Studies of Alkyl-Imidazolium Salts and Their Application in Nanocomposites. *Thermochim. Acta* **2004**, *409*, 3−11.
(24) Garcia, S. J. Effect of Polymer Architecture on the Intrinsic Self-Healing Character of Polymers. *Eur. Polym. J.* **2014**, *53*, 118−125.
(25) Wool, R. P.; O'Connor, K. M. A Theory Crack Healing in Polymers. *J. Appl. Phys.* **1981**, *52*, 5953−5963.
(26) Scheltjens, G.; Diaz, M. M.; Brancart, J.; Van Assche, G.; Van Mele, B. A Self-Healing Polymer Network Based on Reversible Covalent Bonding. *React. Funct. Polym.* **2013**, *73*, 413−420.
(27) Li, Q.; Zhou, H.; Hoyle, C. E. The Effect of Thiol and Ene Structures on Thiol−Ene Networks: Photopolymerization, Physical, Mechanical and Optical Properties. *Polymer* **2009**, *50*, 2237−2245.
(28) Rahman, M. T.; Barikbin, Z.; Badruddoza, A. Z. M.; Doyle, P. S.; Khan, S. A. Monodisperse Polymeric Ionic Liquid Microgel Beads with Multiple Chemically Switchable Functionalities. *Langmuir* **2013**, *29*, 9535−9543.
(29) Vasylevska, G. S.; Borisov, S. M.; Krause, C.; Wolfbeis, O. S. Indicator-Loaded Permeation-Selective Microbeads for Use in Fiber Optic Simultaneous Sensing of Ph and Dissolved Oxygen. *Chem. Mater.* **2006**, *18*, 4609−4616.
(30) Dong, S.; Luo, M.; Peng, G.; Cheng, W. Broad Range Ph Sensor Based on Sol−Gel Entrapped Indicators on Fibre Optic. *Sens. Actuators, B* **2008**, *129*, 94−98.
(31) Spath, A.; Minami, H.; Suzuki, T.; Fink, R. H. Morphology Changes of Ionic Liquid Encapsulating Polymer Microcontainers Upon X-Ray Irradiation. *RSC Adv.* **2014**, *4*, 3272−3277.
(32) Yang, W. W.; Lu, Y. C.; Xiang, Z. Y.; Luo, G. S. Monodispersed Microcapsules Enclosing Ionic Liquid of 1-Butyl-3-Methylimidazolium Hexafluorophosphate. *React. Funct. Polym.* **2007**, *67*, 81−86.
(33) Rana, R. K.; Murthy, V. S.; Yu, J.; Wong, M. S. Nanoparticle Self-Assembly of Hierarchically Ordered Microcapsule Structures. *Adv. Mater.* **2005**, *17*, 1145−1150.
(34) Xiang, Z. Y.; Lu, Y. C.; Zou, Y.; Gong, X. C.; Luo, G. S. Preparation of Microcapsules Containing Ionic Liquids with a New Solvent Extraction System. *React. Funct. Polym.* **2008**, *68*, 1260−1265.
(35) Wei, H.; Wang, Y.; Guo, J.; Shen, N. Z.; Jiang, D.; Zhang, X.; Yan, X.; Zhu, J.; Wang, Q.; Shao, L.; Lin, H.; Wei, S.; Guo, Z. Advanced Micro/Nanocapsules for Self-Healing Smart Anticorrosion Coatings. *J. Mater. Chem. A* **2015**, *3*, 469−480.
(36) Ohno, H.; Yoshizawa, M.; Ogihara, W. Development of New Class of Ion Conductive Polymers Based on Ionic Liquids. *Electrochim. Acta* **2004**, *50*, 255−261.
(37) Subianto, S.; Mistry, M. K.; Choudhury, N. R.; Dutta, N. K.; Knott, R. Composite Polymer Electrolyte Containing Ionic Liquid and Functionalized Polyhedral Oligomeric Silsesquioxanes for Anhydrous Pem Applications. *ACS Appl. Mater. Interfaces* **2009**, *1*, 1173−1182.

DOI: 10.1021/acsami.5b04405
ACS Appl. Mater. Interfaces 2015, 7, 17298−17306